Automated computation of spin- and colour-correlated Born matrix elements

S. Weinzierl[a]

Institut für Physik, Universität Mainz, 55099 Mainz, Germany

Abstract. I report on an implementation of an algorithm for the automated numerical calculation of spin- and colour-correlated Born matrix elements in QCD. These spin- and colour-correlated matrix elements are needed for NLO calculations in combination with the subtraction method. Both massless and massive quarks are considered. There are no restrictions on the number of external particles. As a trivial sub-case, the algorithm also applies to Born matrix elements without any correlations. These are sufficient for leading order calculations.

1 Introduction

QCD processes will constitute the bulk of events at the LHC. These processes provide information on the strong interaction and form quite often important background for searches of new physics. An accurate description of jet physics is therefore mandatory. Although jet observables can rather easily be modelled at leading order (LO) in perturbation theory [1–11], this description suffers several drawbacks. A leading order calculation depends strongly on the renormalisation scale and can therefore give only an order-of-magnitude-estimate on absolute rates. Secondly, at leading order a jet is modelled by a single parton. This is a very crude approximation and oversimplifies inter- and intra-jet correlations. The situation is improved by including higher order corrections in perturbation theory.

At present, there are many next-to-leading order (NLO) calculations for $2 \to 2$ processes at hadron colliders, but only a few for $2 \to 3$ processes. Fully differential numerical programs exist for example for $pp \to 3$ jets [12–14], $pp \to V + 2$ jets [15], $pp \to t\bar{t}H$ [16,17] and $pp \to H + 2$ jets [18,19].

It is desirable to have NLO calculations for $2 \to n$ processes in hadron–hadron collisions with n in the range of $n = 3, 4, ..., 6, 7$. QCD processes like $pp \to n$ jets form often important backgrounds for the search of signals of new physics. However, the complexity of the calculation increases with the number of final-state particles. To overcome the computational limitation, there have been in the past years several proposals for the automated computation of next-to-leading order observables [20–34]. These publications focussed mainly on the automated computation of loop integrals. Equally important is the computation of the real emission contribution. It is well known that in general an NLO observable will receive contributions from the virtual corrections and the real emission part. Taken separately, each of the two contributions is divergent due to the presence of infrared singularities. Only the sum of the two is finite. There are several general method available to handle this problem, like the phase-space slicing method [35–37] or the subtraction method [38–43]. In this paper I will focus on the dipole subtraction method [39–43]. The dipole subtraction method requires the calculation of spin- and colour-correlated Born matrix elements. In this paper I describe a method for the automated calculation of these quantities. While the kinematical part of the matrix elements is calculated numerically, colour-correlation matrices are calculated symbolically at the initialisation phase of the program. The C++ library "GiNaC" [44] allows one to mix numerical and symbolical code in a single program. The program uses standard techniques like spinor methods [45–49] and colour decomposition [50–56]. The program computes helicity amplitudes, which are decomposed into colour factors and partial amplitudes. The partial amplitudes are computed with the help of Berends–Giele type recurrence relations [1,57]. It should be noted that recently interesting new methods emerged for the computation of partial amplitudes [58–61].

This paper is organised as follows: In the following section I present the general setup for the dipole subtraction method and review a few basic tools for the calculation of QCD amplitudes. Section 3 describes the algorithm for the calculation of colour-correlated Born matrix elements. The numerical implementation is discussed in Sect. 4. Finally, Sect. 5 contains the conclusions and an outlook. In an appendix I summarise the colour-ordered Feynman rules and the colour- correlation operators. Furthermore, I give some technical details on the implementation into a C++ program.

ᵃ e-mail: stefanw@thep.physik.uni-mainz.de

2 General setup and basic tools

2.1 The dipole formalism

The starting point for the calculation of an infrared safe observable O in hadron–hadron collisions is the following formula:

$$
\langle O \rangle = \int \mathrm{d}x_1 f(x_1) \int \mathrm{d}x_2
$$
$$
\times f(x_2) \frac{1}{2K(\hat{s})} \frac{1}{(2J_1+1)} \frac{1}{(2J_2+1)} \frac{1}{n_1 n_2}
$$
$$
\times \int \mathrm{d}\phi_n \left(p_1, p_2; p_3, ..., p_{n+2}\right)
$$
$$
\times O\left(p_1, ..., p_{n+2}\right) |\mathcal{A}_{n+2}|^2 . \quad (1)
$$

This equation gives the contribution from the n-parton final state. The two incoming particles are labelled p_1 and p_2, while p_3 to p_{n+2} denote the final-state particles. $f(x)$ gives the probability of finding a parton a with momentum fraction x inside the parent hadron h. A sum over all possible partons a is understood implicitly. $2K(s)$ is the flux factor, $1/(2J_1+1)$ and $1/(2J_2+1)$ correspond to an averaging over the initial helicities and n_1 and n_2 are the number of colour degrees of the initial-state particles. $\mathrm{d}\phi_n$ is the phase-space measure for n final-state particles, including (if appropriate) the identical particle factors. The matrix element $|\mathcal{A}_{n+2}|^2$ is calculated perturbatively.

At NLO one has the following contributions:

$$
\langle O \rangle^{\mathrm{NLO}} = \int_{n+1} O_{n+1} \mathrm{d}\sigma^{\mathrm{R}} + \int_n O_n \mathrm{d}\sigma^{\mathrm{V}} + \int_n O_n \mathrm{d}\sigma^{\mathrm{C}}. \quad (2)
$$

Here I used a rather condensed notation. $\mathrm{d}\sigma^{\mathrm{R}}$ denotes the real emission contribution, whose matrix element is given by the square of the Born amplitudes with $(n+3)$ partons $|\mathcal{A}_{n+3}^{(0)}|^2$. $\mathrm{d}\sigma^{\mathrm{V}}$ gives the virtual contribution, whose matrix element is given by the interference term of the one-loop amplitude $\mathcal{A}_{n+2}^{(1)}$ with $(n+2)$ partons with the corresponding Born amplitude $\mathcal{A}_{n+2}^{(0)}$. $\mathrm{d}\sigma^{\mathrm{C}}$ denotes a collinear subtraction term, which subtracts the initial-state collinear singularities. Taken separately, the individual contributions are divergent and only their sum is finite. In order to render the individual contributions finite, such that the phase-space integrations can be performed by Monte Carlo methods, one adds and subtracts a suitable chosen piece [39–43]:

$$
\langle O \rangle^{\mathrm{NLO}} = \int_{n+1} \left(O_{n+1} \mathrm{d}\sigma^{\mathrm{R}} - O_n \mathrm{d}\sigma^{\mathrm{A}} \right)
$$
$$
+ \int_n \left(O_n \mathrm{d}\sigma^{\mathrm{V}} + O_n \mathrm{d}\sigma^{\mathrm{C}} + O_n \int_1 \mathrm{d}\sigma^{\mathrm{A}} \right). \quad (3)
$$

The matrix element corresponding to the approximation term $\mathrm{d}\sigma^{\mathrm{A}}$ is given as a sum over dipoles:

$$
\sum_{\text{pairs } i,j} \sum_{k \neq i,j} \mathcal{D}_{ij,k}. \quad (4)
$$

Each dipole contribution has the following form:

$$
\mathcal{D}_{ij,k} = -\frac{1}{2p_i \cdot p_j} \mathcal{A}_{n+2}^{(0)\,*} \left(p_1, ..., \tilde{p}_{(ij)}, ..., \tilde{p}_k, ...\right)
$$
$$
\times \frac{\mathbf{T}_k \cdot \mathbf{T}_{ij}}{\mathbf{T}_{ij}^2} V_{ij,k} \mathcal{A}_{n+2}^{(0)} \left(p_1, ..., \tilde{p}_{(ij)}, ..., \tilde{p}_k, ...\right). (5)
$$

Here $\mathbf{T}_i$ denotes the colour charge operator [39] for parton i and $V_{ij,k}$ is a matrix in the spin space of the emitter parton (ij). Explicit formulae for the expressions $V_{ij,k}$ can be found in the literature [39–43] and are not repeated here. In the numerical program both the dipole terms for massless and massive partons are implemented.

In general, the operators $\mathbf{T}_i$ lead to colour correlations, while the $V_{ij,k}$ lead to spin correlations. The colour charge operators $\mathbf{T}_i$ for a quark, gluon and antiquark in the final state are

$$
\text{quark}: \quad \mathcal{A}^* (...q_i...) \left(T_{ij}^a\right) \mathcal{A} (...q_j...),
$$
$$
\text{gluon}: \quad \mathcal{A}^* (...g^c...) \left(\mathrm{i}f^{cab}\right) \mathcal{A} (...g^b...),
$$
$$
\text{antiquark}: \quad \mathcal{A}^* (...\bar{q}_i...) \left(-T_{ji}^a\right) \mathcal{A} (...\bar{q}_j...). \quad (6)
$$

The corresponding colour charge operators for a quark, gluon and antiquark in the initial state are

$$
\text{quark}: \quad \mathcal{A}^* (...\bar{q}_i...) \left(-T_{ji}^a\right) \mathcal{A} (...\bar{q}_j...),
$$
$$
\text{gluon}: \quad \mathcal{A}^* (...g^c...) \left(\mathrm{i}f^{cab}\right) \mathcal{A} (...g^b...),
$$
$$
\text{antiquark}: \quad \mathcal{A}^* (...q_i...) \left(T_{ij}^a\right) \mathcal{A} (...q_j...). \quad (7)
$$

In the amplitude an incoming quark is denoted as an outgoing antiquark and vice versa.

The subtraction term can be integrated over the unresolved one-parton phase space. Due to this integration, all spin correlations average out, but colour correlations still remain. In a compact notation, the result of this integration is often written as

$$
\mathrm{d}\sigma^{\mathrm{C}} + \int_1 \mathrm{d}\sigma^{\mathrm{A}} = \mathbf{I} \otimes \mathrm{d}\sigma^{\mathrm{B}} + \mathbf{K} \otimes \mathrm{d}\sigma^{\mathrm{B}} + \mathbf{P} \otimes \mathrm{d}\sigma^{\mathrm{B}}. \quad (8)
$$

The notation $\otimes$ indicates that colour correlation still remains. The term $\mathbf{I} \otimes \mathrm{d}\sigma^{\mathrm{B}}$ lives on the phase space of the n-parton configuration and has the appropriate singularity structure to cancel the infrared divergences coming from the one-loop amplitude. Therefore $\mathrm{d}\sigma^{\mathrm{V}} + \mathbf{I} \otimes \mathrm{d}\sigma^{\mathrm{B}}$ is infrared finite.

The purpose of the paper is to set up a numerical program for the automated computation of the terms

$$
\int_{n+1} \left(O_{n+1} \mathrm{d}\sigma^{\mathrm{R}} - O_n \mathrm{d}\sigma^{\mathrm{A}} \right) \quad (9)
$$

and

$$
\int_n O_n \left(\mathbf{I} \otimes \mathrm{d}\sigma^{\mathrm{B}} + \mathbf{K} \otimes \mathrm{d}\sigma^{\mathrm{B}} + \mathbf{P} \otimes \mathrm{d}\sigma^{\mathrm{B}} \right). \quad (10)
$$

This requires the computation of the matrix elements with $(n+3)$ partons with no spin or colour correlations (implicit

in $d\sigma^R$) as well as the computation of matrix elements with $(n+2)$ partons with spin and colour correlations. The subtraction terms in (9) involve spin and colour correlations. The insertion operators **I**, **K** and **P** induce colour correlations, but no spin correlations. One is therefore naturally lead to the calculation of colour-ordered amplitudes in a helicity basis. Basic techniques for such a task are reviewed in the next subsections.

2.2 Double line notation

In QCD one deals with quarks and gluons. Both types of partons carry information on the colour degrees of freedoms and the kinematical degrees of freedom. Quarks have a colour index i, running from 1 to N and corresponding to the fundamental representation of $SU(N)$. The kinematical information can be represented for massless quarks by Weyl spinors p_A or $p_{\dot{B}}$, where the indices A or $\dot{B}$ run from 1 to 2. The corresponding information for gluons is in the conventional approach represented by a colour index a, running from 1 to $N^2 - 1$ and which corresponds to the adjoint representation of $SU(N)$. The kinematical information is represented by a Lorentz index μ, running from 0 to 3. It is useful, to treat quarks and gluons on the same footing. To this aim, I follow the "double-line" approach [62] and convert a gluon index to two quark indices. I do this for the colour degrees of freedom, as well as for the kinematical parts.

In detail, this is done as follows: In Feynman diagrams one distinguishes edges and vertices. Edges are propagators as well as polarisation vectors or spinors for external particles. Vertices are all interaction vertices. For vector-like couplings one can write

$$V_\mu E^\mu = V_\mu g^{\mu\nu} E_\nu = V_\mu \left(\frac{1}{2} \sigma^\mu_{A\dot{B}} \bar{\sigma}^{\nu \dot{B} A} \right) E_\nu \qquad (11)$$

$$= \left(\frac{1}{\sqrt{2}} V_\mu \sigma^\mu_{A\dot{B}} \right) \left(\frac{1}{\sqrt{2}} \bar{\sigma}^{\nu \dot{B} A} E_\nu \right),$$

which allows us to replace a contraction over μ by two contractions over A and $\dot{B}$. One can apply the same trick to the colour algebra:

$$V^a E^a = V^a \delta^{ab} E^b = V^a \left(2 T^a_{ij} T^b_{ji} \right) E^b$$
$$= \left(\sqrt{2} T^a_{ij} V^a \right) \left(\sqrt{2} T^b_{ji} E^b \right). \qquad (12)$$

Again, this equation allows us to replace a contraction over an adjoint index a by two contractions over indices i and j in the fundamental representation. The Feynman rules for QCD in the double line notation are listed in Appendix A.

2.3 Colour decomposition

In this paper I use the normalisation

$$\text{Tr } T^a T^b = \frac{1}{2} \delta^{ab} \qquad (13)$$

for the colour matrices. Amplitudes in QCD may be decomposed into group-theoretical factors (carrying the colour structures) multiplied by kinematic functions called partial amplitudes [50–54]. These partial amplitudes do not contain any colour information and are gauge-invariant objects.

The colour decomposition is obtained by replacing the structure constants f^{abc} by

$$\mathrm{i} f^{abc} = 2 \left[\text{Tr} \left(T^a T^b T^c \right) - \text{Tr} \left(T^b T^a T^c \right) \right], \qquad (14)$$

which follows from $\left[T^a, T^b \right] = \mathrm{i} f^{abc} T^c$. The resulting traces and strings of colour matrices can be further simplified with the help of the Fierz identity:

$$T^a_{ij} T^a_{kl} = \frac{1}{2} \left(\delta_{il} \delta_{jk} - \frac{1}{N} \delta_{ij} \delta_{kl} \right). \qquad (15)$$

In the pure gluonic case tree level amplitudes with n external gluons may be written in the form

$$\mathcal{A}_n(1, 2, ..., n) \qquad (16)$$
$$= \left(\frac{g}{\sqrt{2}} \right)^{n-2} \sum_{\sigma \in S_n / Z_n} \delta_{i_{\sigma_1} j_{\sigma_2}} \delta_{i_{\sigma_2} j_{\sigma_3}} ... \delta_{i_{\sigma_n} j_{\sigma_1}} A_n \left(\sigma_1, ..., \sigma_n \right),$$

where the sum is over all non-cyclic permutations of the external gluon legs. The quantities $A_n(\sigma_1, ..., \sigma_n)$, called the partial amplitudes, contain the kinematic information. They are colour-ordered, e.g. only diagrams with a particular cyclic ordering of the gluon s contribute. The choice of the basis for the colour structures is not unique, and several proposals for bases can be found in the literature [55,56]. Here I use the "colour-flow decomposition" [56]. As a further example I give the colour decomposition for a tree amplitude with a pair of quarks:

$$\mathcal{A}_{n+2}(q, 1, 2, ..., n, \bar{q})$$
$$= \left(\frac{g}{\sqrt{2}} \right)^n \sum_{S_n} \delta_{i_q j_{\sigma_1}} \delta_{i_{\sigma_1} j_{\sigma_2}} ... \delta_{i_{\sigma_n} j_{\bar{q}}}$$
$$\times A_{n+2}(q, \sigma_1, \sigma_2, ..., \sigma_n, \bar{q}). \qquad (17)$$

where the sum is over all permutations of the gluon legs. In squaring these amplitudes a colour projector

$$\delta_{\bar{i}i} \delta_{j\bar{j}} - \frac{1}{N} \delta_{i\bar{j}} \delta_{j\bar{i}} \qquad (18)$$

has to applied to each gluon.

While the colour structure of the examples quoted above is rather simple, the colour decomposition can be become rather involved for amplitudes with many pairs of quarks. A systematic algorithm for the colour decomposition and the diagrams contributing to a single colour structure is given in Sect. 3.

2.4 Spinor techniques

For the calculation of helicity amplitudes [45–49] one chooses for the spinors corresponding to external massless quarks two-component Weyl spinors. Two notations
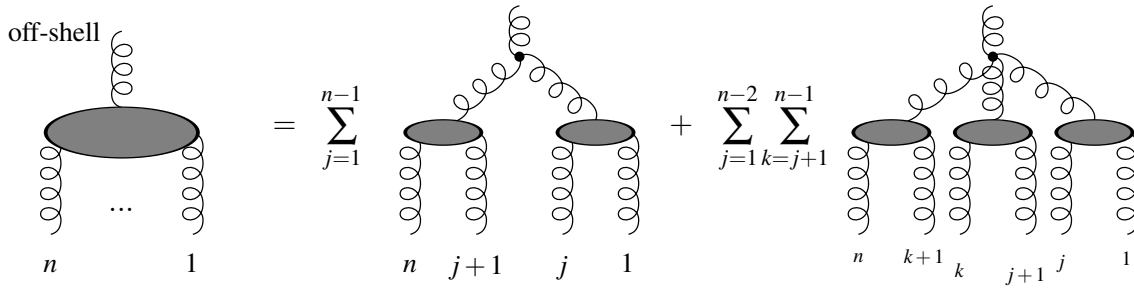
Fig. 1. The recurrence relation for the gluon current. An off-shell current with n legs can be computed recursively from off-shell currents with fewer legs

for Weyl spinors are commonly used in the literature. The relation between the bra-ket notation and the notation using dotted and undotted indices is as follows:

$$|p+\rangle = p_B, \quad \langle p+| = p_{\dot{A}}, \tag{19}$$

$$|p-\rangle = p^{\dot{B}}, \quad \langle p-| = p^A. \tag{20}$$

Spinor products are denoted as follows:

$$\langle pq\rangle = \langle p-|q+\rangle = p^A q_A, \quad [qp] = \langle q+|p-\rangle = q_{\dot{A}} p^{\dot{A}}. \tag{21}$$

For the polarisation vectors of the external gluons one uses

$$\varepsilon_\mu^+(k,q) = \frac{\langle q-|\gamma_\mu|k-\rangle}{\sqrt{2}\langle q-|k+\rangle}, \quad \varepsilon_\mu^-(k,q) = \frac{\langle q+|\gamma_\mu|k+\rangle}{\sqrt{2}\langle k+|q-\rangle}, \tag{22}$$

where k is the momentum of the gluon and q is an arbitrary light-like reference momentum. In the "double-line" notation this becomes

$$\varepsilon_+^{\dot{A}B}(k,q) = \frac{1}{\langle qk\rangle} k^{\dot{A}} q^B, \quad \varepsilon_-^{\dot{A}B}(k,q) = \frac{1}{[kq]} q^{\dot{A}} k^B. \tag{23}$$

For spinors corresponding to massive quarks the formulae from [63] are used.

2.5 Recurrence relations

Recursive techniques [1,57] build partial amplitudes from smaller building blocks, usually called colour-ordered off-shell currents. Off-shell currents are objects with n on-shell legs and one additional leg off-shell. Momentum conservation is satisfied. It should be noted that off-shell currents are not gauge-invariant objects. Recurrence relations relate off-shell currents with n legs to off-shell currents with fewer legs.

For the pure gluon current $J_n^{\dot{A}B}$, the recurrence relation reads

$$J_n^{\dot{A}B}\left(p_1^\pm, ..., p_n^\pm; q_1, ..., q_n\right)$$
$$= \sum_{j=1}^{n-1} J_j^{\dot{C}D}\left(p_1^\pm, ..., p_j^\pm; q_1, ..., q_j\right)$$

$$\times J_{n-j}^{\dot{E}F}\left(p_{j+1}^\pm, ..., p_n^\pm; q_{j+1}, ..., q_n\right)$$
$$\times V_{D\dot{C}F\dot{E}H\dot{G}}(p_{1,j}, p_{j+1,n}) P^{\dot{G}H\dot{A}B}(p_{1,n})$$
$$+ \sum_{j=1}^{n-2} \sum_{k=j+1}^{n-1} J_j^{\dot{C}D}\left(p_1^\pm, ..., p_j^\pm; q_1, ..., q_j\right)$$
$$\times J_{k-j}^{\dot{E}F}\left(p_{j+1}^\pm, ..., p_k^\pm; q_{j+1}, ..., q_k\right)$$
$$\times J_{n-k}^{\dot{G}H}\left(p_{k+1}^\pm, ..., p_n^\pm; q_{k+1}, ..., q_n\right)$$
$$\times V_{D\dot{C}F\dot{E}H\dot{G}J\dot{I}} P^{\dot{I}J\dot{A}B}(p_{1,n}). \tag{24}$$

This relation is pictorially shown in Fig. 1. In this formula, the q_i are the reference momenta for the external gluons, $P^{\dot{C}D\dot{A}B}(k)$ is the expression for the gluon propagator and $V_{B\dot{A}D\dot{C}F\dot{E}}(k_1, k_2)$ and $V_{B\dot{A}D\dot{C}F\dot{E}H\dot{G}}$ are the expressions for the three-gluon and four-gluon vertices, respectively. I further used the notation

$$p_{i,j} = \sum_{l=i}^{j} p_l. \tag{25}$$

The recursion starts with the current with one external leg, which is given by the polarisation vector:

$$J_1^{\dot{A}B}\left(p_1^\pm; q_1\right) = \varepsilon_\pm^{\dot{A}B}(p_1, q_1). \tag{26}$$

Similar recurrence relations can be written down for the quark and antiquark currents, as well as the gluon currents in full QCD. The guiding principle is to follow the off-shell leg into the "blob", representing the sum of all diagrams, and to sum on the RHS of the recurrence relation over all vertices involving this off-shell leg and off-shell currents with less external legs.

3 The method

In this section I describe in detail the method for the automated computation of Born matrix elements in QCD. The matrix elements may or may not involve spin and/or colour correlations.

3.1 Helicity amplitudes and spin correlations

The program computes helicity amplitudes. For a given set of external momenta, each helicity amplitude evaluates to

a complex number. If no spin correlations are present, the matrix element is simply given as the squared modulus of the amplitude summed over all helicity configurations. In the dipole formalism, spin correlations are related to the splittings $g \to gg$ and $g \to q\bar{q}$. In the original formulation of Catani and Seymour they are written as

$$\mathcal{A}_\mu^* \left(..., p_{(ij)}, ...\right) S^{\mu\nu} \mathcal{A}_\nu \left(..., p_{(ij)}, ...\right), \qquad (27)$$

where $\mathcal{A}_\mu$ denotes the amplitude with the polarisation vector of the emitter gluon (ij) amputated. Furthermore, the spin correlation tensor is of the form

$$S^{\mu\nu} = v^\mu v^\nu, \qquad (28)$$

and the vector v^μ satisfies

$$v \cdot p_{(ij)} = 0. \qquad (29)$$

Within the helicity formalism the spin correlation is evaluated as [64]

$$\mathcal{A}_\mu^* S^{\mu\nu} \mathcal{A}_\nu = \left| E \mathcal{A} \left(..., p_{(ij)}^+, ...\right) + E^* \mathcal{A} \left(..., p_{(ij)}^-, ...\right) \right|^2, \qquad (30)$$

where $\mathcal{A}(..., p_{(ij)}^\pm, ...)$ denotes the helicity amplitude, where the emitter gluon has "+", respectively "−" helicity. E is given by

$$E = \varepsilon_-^\mu v_\mu = \frac{\langle q + |v| p_{(ij)} + \rangle}{\sqrt{2} \left[p_{(ij)} q\right]}. \qquad (31)$$

In (31) q is as usual an arbitrary null reference momentum.

3.2 Amplitudes with more than one quark–antiquark pair

If more than one quark–antiquark pair is present, we have to sum over all quark permutations. An amplitude with n_q quark–antiquark pairs can be written as

$$\mathcal{A} \left(\bar{q}_1, q_1, ..., \bar{q}_2, q_2, ..., \bar{q}_{n_q}, q_{n_q}\right)$$
$$= \sum_{\sigma \in S(n_q)} (-1)^\sigma \left(\prod_{j=1}^{n_q} \delta_{\bar{q}_j q_{\sigma(j)}}^{\text{flav}}\right)$$
$$\times \hat{\mathcal{A}} \left(\bar{q}_1, q_{\sigma(1)}, ..., \bar{q}_2, q_{\sigma(2)}, ..., \bar{q}_{n_q}, q_{\sigma(n_q)}\right). \qquad (32)$$

Here, $(-1)^\sigma$ equals -1 whenever the permutation is odd and equals $+1$ if the permutation is even. In $\hat{\mathcal{A}}$ each external quark–antiquark pair $(\bar{q}_j, q_{\sigma(j)})$ is connected by a continuous fermion line. The flavour factor $\delta_{\bar{q}_j q_{\sigma(j)}}^{\text{flav}}$ ensures that this combination is only taken into account if $\bar{q}_j$ and $q_{\sigma(j)}$ have the same flavour.

3.3 The colour structure

The amplitude $\hat{\mathcal{A}}$ is decomposed into colour factors and partial amplitudes:

$$\hat{\mathcal{A}} = \sum_i c_i A_i. \qquad (33)$$

Each partial amplitude A_i has a fixed cyclic ordering of the external legs. For Born graphs we can take this ordering such that a quark follows immediately its corresponding antiquark in the clockwise orientation. This is shown in Fig. 2.

That is to say, gluons are emitted from a quark line only to the right when following the fermion line arrow. If a gluon would be emitted to the left, we could draw an equivalent diagram by flipping the off-shell current attached to this gluon to the right of the fermion line.

All possible cyclic orderings are generated as follows: We assume that the amplitude has n_g external gluons, n_q external quarks and therefore necessarily also n_q external antiquarks. We first note, since a quark follows immediately its corresponding antiquark, we can treat an adjacent $(\bar{q}, q)$-pair as an external "pseudo-leg", which is permutated together. The amplitude has therefore $n_g + n_q$ pseudo-legs. Then all possible cyclic orderings are obtained by summing over all permutations of the pseudo-legs and factoring out the cyclic permutations, e.g. each ordering corresponds to an element of

$$S(n_g + n_q)/Z(n_g + n_q). \qquad (34)$$

This is equivalent to fixing the first external pseudo-leg and summing over all permutation of the remaining $(n_g + n_q - 1)$ external pseudo-legs. Therefore there are
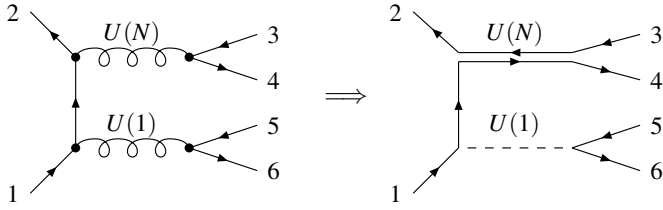
$$(n_g + n_q - 1)! \qquad (35)$$

inequivalent cyclic orderings.

For the pure gluon amplitude $(n_q = 0)$ each cyclic ordering corresponds to one colour factor c_i. The situation is different if quarks are present $(n_q \neq 0)$. This is related
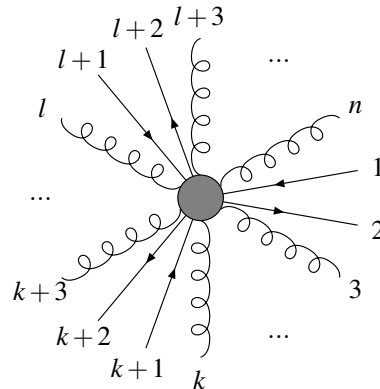
Fig. 2. The cyclic order of a partial amplitude. Without loss of generality we can assume that quarks follow immediately antiquarks in the clockwise order

Fig. 3. An example for the decomposition into colour clusters

to the fact that the gluon propagator in an $SU(N)$ gauge theory can be written as a propagator corresponding to an $U(N)$ gauge theory minus a part which subtracts out the additional $U(1)$ piece. The kinematic parts of the $U(n)$ and the $U(1)$ pieces are the same:

$$P^{\dot{B}A\dot{D}C}(k) = \quad \dot{B}A \quad \text{OOOOO} \quad \dot{D}C$$
$$= \frac{\mathrm{i}}{k^2}\left(-\varepsilon^{\dot{B}\dot{D}}\varepsilon^{AC}\right), \qquad (36)$$

However, they differ by their colour structure:

$$U(N): \quad \begin{matrix} i & \xrightarrow{\quad\quad} & l \\ j & \xrightarrow{\quad\quad} & k \end{matrix} = \delta_{il}\delta_{kj},$$

$$U(1): \quad \begin{matrix} i \\ j \end{matrix} \dashleftarrow - - - \dashrightarrow \begin{matrix} l \\ k \end{matrix} = -\frac{1}{N}\delta_{ij}\delta_{kl}. \qquad (37)$$

Note that each propagation of a $U(1)$ gluon is accompanied by a factor $(-1)/N$. It can be shown that the $U(1)$ gluon couples only to quark lines [56]. Therefore an amplitude with n_q quarks can contain up to $(n_q - 1)$ gluons of type $U(1)$. Each $U(1)$ gluon separates a Born amplitude into colour-disconnected pieces. We define a colour cluster as a part of an amplitude, which is connected to the rest of the amplitude only by an $U(1)$ gluon and which does not contain by itself any $U(1)$ gluon. This concept is illustrated in Fig. 3, which shows a diagram with three quark–antiquark pairs, one $U(N)$ gluon and one $U(1)$ gluon. This diagram has two colour clusters, formed by the particles $(1, 2, 3, 4)$ and $(5, 6)$, and separated by the $U(1)$ gluon. For an amplitude with n_q quark–antiquark pairs one can have from 1 to n_q colour clusters. From the cluster decomposition the colour structure can be read off easily. The example in Fig. 3 contributes to the colour structure

$$\left(-\frac{1}{N}\right)(\delta_{i_2 j_3}\delta_{i_4 j_1})(\delta_{i_6 j_5}). \qquad (38)$$

In general, given a colour cluster assignment, the corresponding colour factor c_i is constructed as follows: First of all, the colour factor factorizes into a product of the contributions from the individual colour clusters.

$$c_i = \left(-\frac{1}{N}\right)^{(n_{\mathrm{cluster}}-1)} \times \prod_{j=1}^{n_{\mathrm{cluster}}} c_{i,j}. \qquad (39)$$

$c_{i,j}$ is the colour factor corresponding to cluster j. For a cluster consisting only of gluons, $c_{i,j}$ is given by

$$g_1, g_2, ..., g_n: \quad c_{i,j} = \delta_{i_1 j_2}\delta_{i_2 j_3}...\delta_{i_{n-1} j_n}\delta_{i_n j_1}. \qquad (40)$$

An antiquark–quark pair can be treated effectively as a single gluon. For example the colour factor associated to a colour cluster consisting of an quark–antiquark pair and $(n-2)$ gluons is given by

$$\bar{q}_1, q_2, g_3, ..., g_n: \quad c_{i,j} = \delta_{i_2 j_3}\delta_{i_3 j_4}...\delta_{i_{n-1} j_n}\delta_{i_n j_1}. \qquad (41)$$

As a further example we quote the colour factor for a cluster with two quark- antiquark pairs:

$$\bar{q}_1, q_2, g_3, ..., \bar{q}_k, q_{k+1}, ..., g_n:$$
$$c_{i,j} = \delta_{i_2 j_3}\delta_{i_3 j_4}...\delta_{i_{k-1} j_k}\delta_{i_{k+1} j_{k+2}}...\delta_{i_{n-1} j_n}\delta_{i_n j_1}. \qquad (42)$$

The pattern should be clear. The colour factor associated to a individual colour cluster is just a sequence of Kronecker δs, corresponding to the cyclic ordering of the legs belonging to this colour cluster.

It remains to derive a method, how all possible colour clusterings can be generated. This is a combinatorial problem. For a fixed cyclic ordering we can generate all possible colour clusterings as follows: We first sum over the number of possible colour clusters. Let n_{cluster} be the number of colour clusters, where n_{cluster} ranges from 1 to n_q. For a fixed n_{cluster} we then sum over all partitions of $(n_g + n_q)$ into n_{cluster} pieces n_j^{cluster}, such that

$$\sum_{j=1}^{n_{\mathrm{cluster}}} n_j^{\mathrm{cluster}} = n_g + n_q. \qquad (43)$$

For a partition we take into account the order, such that for example $(1, 1, 2)$, $(1, 2, 1)$ and $(2, 1, 1)$ are distinct partitions of 4. n_j^{cluster} gives the number of external pseudo-legs belonging to cluster j. Obviously, an adjacent antiquark–quark pair has to belong to the same colour cluster, therefore it is counted as one external pseudo-leg. Finally, we have to sum over all possible starting points of the colour clusters with respect to the cyclic ordering. Here we observe that the members of a colour cluster need not be adjacent in the cyclic ordering. An example for a colour assignment in the cyclic ordering would be

$$\underbrace{(\bar{q}, q), g, g}_{\text{cluster 1}}, \underbrace{g, (\bar{q}, q), g}_{\text{cluster 2}}, \underbrace{g, g, g, g}_{\text{cluster1}}, \underbrace{g, (\bar{q}, q), g, g}_{\text{cluster 3}}. \qquad (44)$$

In this example, cluster 2 is embedded in cluster 1. The summation over the starting points has to fulfill the following requirements.
(i) The external pseudo-leg 1 belongs to colour cluster 1.
(ii) The colour cluster $(j+1)$ starts after colour cluster j for all $j > 2$. (Colour cluster 1 may start at the end of the cyclic ordering.)
(iii) If the assignment of external pseudo-legs to colour cluster j has been interrupted by the starting of a new cluster k (with $k > j$), the assignment to cluster j cannot be continued until all members of cluster k have been assigned.

Requirement (iii) ensures that we cannot have a sequence like cluster 1, cluster 2, cluster 1, cluster 2. The assignment of the external pseudo-legs to colour clusters is now done as follows: Let

$$\left(m_2^{\mathrm{start}}, m_3^{\mathrm{start}}, ..., m_{n_{\mathrm{cluster}}}^{\mathrm{start}}\right) \qquad (45)$$

be an $(n_\text{cluster} - 1)$-tuple, such that

$$m_j^\text{start} \leq m_{j+1}^\text{start} \qquad (46)$$

and

$$1 \leq m_j^\text{start} \leq 2 - j + \sum_{k=1}^{j-1} n_k^\text{cluster} \qquad (47)$$

Then

$$n_j^\text{start} = m_j^\text{start} + j - 1 \qquad (48)$$

defines the starting point of cluster j for $j = 2, ..., n_\text{cluster}$. The starting points n_j^start together with the rules (i) and (iii) define uniquely the assignment of the external pseudo-legs to the colour clusters. Summing over all $(n_\text{cluster} - 1)$-tuples in (45) subject to the constraints (46) and (47) generates all possibilities with n_cluster colour clusters, in which colour cluster j has n_j^cluster external pseudo-legs.

Since each colour cluster couples to the rest of the amplitude through a $U(1)$-gluon, it has to contain at least one quark–antiquark pair. Therefore configurations, where a colour cluster does not contain a quark–antiquark pair are vetoed, with the trivial exception of the pure gluon amplitude, which consists of one colour cluster and no quark–antiquark pairs.

With the colour cluster decomposition and a method for the generation of all cluster decomposition at hand, I now turn back to the computation of the amplitude squared. From (32) and (33) it is clear that we can write any amplitude in the form

$$\mathcal{A} = \sum_i c_i A_i, \qquad (49)$$

where the c_i are the colour factors and the A_i are the partial amplitudes which contain the kinematical information. In squaring the amplitude we obtain

$$|\mathcal{A}|^2 = \sum_{i,j} A_i \left(c_i P c_j^\dagger \right) A_j^*. \qquad (50)$$

The colour projector is given as a product with one factor for each external particle:

$$P = \prod_{k=1}^{n_g + 2n_q} P_k, \qquad (51)$$

where the individual colour projectors for a quark, antiquark and a gluon are

$$P_q = \delta_{\bar{i}i}, \quad P_{\bar{q}} = \delta_{j\bar{j}}, \quad P_g = \delta_{\bar{i}i}\delta_{j\bar{j}} - \frac{1}{N}\delta_{\bar{i}j}\delta_{ji}. \qquad (52)$$

The only non-trivial piece is given by the colour projector for the external gluons, which is a consequence of the double-line notation. Note that

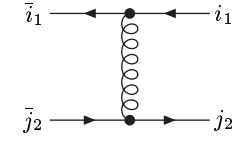$$M_{ij} = \left(c_i P c_j^\dagger \right) \qquad (53)$$

defines a matrix which is independent of the four-momenta of the particles. Therefore this matrix can be calculated at the initialisation phase of the program. As each entry is given as a contraction of Kronecker δs, this can be done easily symbolically with the rules

$$\delta_{ij}\delta_{jk} = \delta_{ik}, \ \ \delta_{ii} = N. \qquad (54)$$

The program uses the C++ library "GiNaC" for this task. In Appendix (B.1) I give a small example program. The resulting expression is a function of N, and after substituting $N = 3$ the result can be converted to a double precision number. Note that run-time performance is not an issue here, since this calculation occurs only at the initialisation phase of the program. To obtain the amplitude squared, the matrix M_{ij} is first calculated at the initialisation phase and stored in memory. Then for each momentum configuration the vector of partial amplitudes $\boldsymbol{A} = (A_1, A_2, ...)$ is computed. The amplitude squared is then given by

$$|\mathcal{A}|^2 = \boldsymbol{A} \, M \, \boldsymbol{A}^\dagger. \qquad (55)$$

The inclusion of colour-correlations is rather straightforward. To include colour-correlation between particles a and b, one replaces P_a and P_b in (51) by the appropriate colour- correlation operator. For example, the colour-correlation operator $\boldsymbol{T}_q \cdot \boldsymbol{T}_{\bar{q}}$ for a quark–antiquark pair reads

$$= -\frac{1}{2} \left(\delta_{\bar{i}_1 \bar{j}_2}\delta_{j_2 i_1} - \frac{1}{N}\delta_{\bar{i}_1 i_1}\delta_{j_2 \bar{j}_2} \right). \qquad (56)$$

A complete list of all relevant colour-correlation operators can be found in Appendix B. The corresponding matrices M_{ij} depend now on a and b but are still independent of the four-momenta of the particles. Therefore they can be computed at the initialisation phase of the program. For a matrix element with $n = n_g + 2n_q$ external particles, there are

$$\frac{1}{2}n(n-1) \qquad (57)$$

possibilities of choosing the colour-correlated partons a and b. Therefore the initialisation phase of the program computes and stores $n(n-1)/2$ different colour matrices M_{ij}. For realistic values of n, say $n < 9$, the CPU time and memory requirements for this task are rather modest.

3.4 The partial amplitudes

It remains to discuss how the partial amplitudes A_i, entering (49) and (50), are computed. This is done with the help of off-shell currents and recurrence relations. Compared to the introductory discussion of the pure gluonic

off-shell current in Sect. 2.5 there are additional complications: First of all, a rather trivial extension is given by the fact that in full QCD we have to allow for the possibility of multiple quark–antiquark pairs. Secondly, and more important, it is a fact that the recurrence relations have to respect the decomposition of a partial amplitude into colour clusters. The algorithm is summarised as follows.

(i) We consider coupled recurrence relations for the off-shell currents corresponding to an $U(N)$-gluon, an $U(1)$-gluon, quarks and antiquarks. Note that the $U(N)$-gluon and the $U(1)$-gluon are treated separately, as the latter couples only to quarks. It is also convenient to distinguish the off-shell currents for the quarks and antiquarks, depending on whether the quarks are massive or massless. In the latter case specialised (and faster) routines can be used, since only helicity conserving interactions enter.

(ii) All recurrence relation express an off-shell current of type A as a sum over off-shell currents with fewer legs, which are combined through the basic three- or four-valent vertices of the theory. The recurrence relations takes into account all possible interaction vertices, which contain A. Note that the off-shell currents, which enter the RHS of the recurrence relation need not be of type A. For the example, the recurrence relation for an $U(N)$-gluon involves the quark–antiquark–gluon vertex and therefore the off-shell currents for a quark and an antiquark. In general, the recurrence relations yield a coupled system of equations.

(iii) The off-shell parton for the quark current, the antiquark current and the $U(N)$-gluon current belong to a specific colour cluster a. The recurrence relation splits the off-shell current with n external legs into off-shell currents with less external legs. This splitting has to respect the following selection rules.

– For the $U(N)$-current, the off-shell current attached through the three- and four-gluon vertex have to contain at least one parton belonging to colour cluster a. In the off-shell quark and antiquark current, which are attached through the gluon–quark–antiquark vertex to the $U(N)$-gluon current, the off-shell quark and antiquark lines have to belong to colour cluster a.

– For the off-shell quark current, the sub-current attached through an $U(N)$-gluon must contain at least one parton belonging to colour cluster a. On the other hand, the sub-current attached through an $U(1)$-gluon may not contain any parton of colour cluster a. Similar considerations apply to the antiquark current.

– Finally, the off-shell $U(1)$-current is rather simple and the recurrence relation involves an quark and an antiquark current, whose off-shell legs necessarily belong to the same colour cluster.

(iv) As a further selection rule we have to veto configurations, where the off-shell current is divided into sub-currents between leg j and $(j+1)$, in the case where these two legs belong to the same colour cluster b, which is different from the colour cluster a of the off-shell leg. That is to say the recurrence relation where the off-shell leg belongs to cluster a cannot split legs which belong to a different colour cluster b.

3.5 The pure gluon amplitude

In principle, the pure gluon amplitude can be treated with the methods discussed above. However the pure gluon amplitude is a rather special case, which leads to many additional simplifications. Since it is known that pure gluonic processes will contribute significantly to the cross section at the LHC, it is desirable to treat these processes separately with optimised routines, taking into account the additional simplifications. The simplifications are as follows.

(1) There is only one colour cluster and the colour decomposition is simply given by the $(n_g-1)!$ inequivalent cyclic orderings, as in (16).

(2) $U(1)$-gluons can be ignored and the recurrence relation for the partial amplitudes is given by (24).

(3) In calculating the colour matrix M_{ij}, the colour projectors P_g in (52) may be replaced by

$$P_g \to \delta_{\bar{i}i}\delta_{j\bar{j}}. \tag{58}$$

3.6 QCD amplitudes with one electro-weak boson

The methods discussed above require only minor modifications to include amplitudes with QCD partons and one electro-weak boson. As these are relevant to electron–positron annihilation, electron–proton collisions or Z-production at the LHC / Tevatron, these amplitudes have been implemented as well. The amplitudes are computed by considering a recurrence relation, which couples the electro-weak current to an off-shell quark current and an off-shell antiquark current.

4 Numerical implementation

The algorithms discussed above have been implemented into a computer program. This numerical program can compute Born matrix elements in QCD with spin and colour correlations. To test the program I have first considered the case where spin and colour correlations are absent. In this case one can compare the results with the ones from the program Madgraph. I quote here the results of this comparison for processes with up to seven external particles. The labelling of the momenta is

$$p_1 p_2 \to p_3, p_4, ..., p_n. \tag{59}$$

p_1 and p_2 are the incoming momenta, p_3 to p_n are the outgoing momenta. For $2 \to 2$ processes I took the following set of momenta (in units of GeV):

$$p_1 = (45.0, 0.0, 0.0, -45.0),$$
$$p_2 = (45.0, 0.0, 0.0, 45.0),$$
$$p_3 = (45.0, -20.8997, -29.6778, 26.5976),$$
$$p_4 = (45.0, 20.8997, 29.6778, -26.5976). \tag{60}$$

The same initial-state momenta p_1 and p_2 are used for all other processes. The final-state momenta for the $2 \to 3$ processes were chosen as

$$p_3 = (41.8145, -9.20663, -26.7503, 30.7914),$$

$$p_4 = (17.3829, 12.8067, 10.7712, -4.70487),$$
$$p_5 = (30.8026, -3.6001, 15.9791, -26.0865). \quad (61)$$

For $2 \to 4$ processes I used

$$p_3 = (29.9152, -18.1846, -8.69254, 22.1061),$$
$$p_4 = (9.82719, 4.07529, 8.79524, -1.61538),$$
$$p_5 = (22.171, -9.26417, 14.187, -14.2988),$$
$$p_6 = (28.0866, 23.3735, -14.2898, -6.19197). \quad (62)$$

Finally, for $2 \to 5$ processes I used

$$p_3 = (20.165, -13.0392, 0.0298292, 15.3819),$$
$$p_4 = (9.60811, 2.4114, 9.15728, -1.6264),$$
$$p_5 = (20.5589, -7.64505, 15.4771, -11.166),$$
$$p_6 = (18.087, 17.056, -3.25968, -5.06046),$$
$$p_7 = (21.581, 1.21688, -21.4045, 2.47093). \quad (63)$$

The strong coupling constant was taken to be $\alpha_s = 0.118$. For this comparison, all quark masses have been set to zero. The flavour labels serve only to distinguish identical quarks from non-identical quarks. Table 1 shows the comparison of our program with Madgraph for the computation of the matrix elements corresponding to the indicated processes. The results do not contain any averaging over the colour degrees of freedom for the initial-state particles, nor do they contain symmetry factors for the final-state particles. As can be seen from the table, the agreement is satisfactory.

To check spin and colour correlations I have compared the program with existing NLO codes for $e^+e^- \to 4$ jets [64] and $pp \to t\bar{t}g$ [65]. Furthermore I checked that the Born matrix elements approach the corresponding subtraction terms in all collinear and soft limits.

Table 1. Comparison of our program with Madgraph for various matrix elements with up to seven external particles

Process	This work	Madgraph
$gg \to gg$	56203.4	56203.2
$g\bar{d} \to \bar{d}g$	8436.64	8436.62
$u\bar{d} \to \bar{d}u$	1374.01	1374.01
$d\bar{d} \to \bar{d}d$	1287.74	1287.74
$gg \to ggg$	21269.2	21269.3
$g\bar{d} \to \bar{d}gg$	3222.01	3222.02
$u\bar{d} \to \bar{d}ug$	56.459	56.4591
$d\bar{d} \to \bar{d}dg$	53.2424	53.2425
$gg \to gggg$	1354.24	1354.22
$g\bar{d} \to \bar{d}ggg$	138.691	138.689
$u\bar{d} \to \bar{d}ugg$	0.975563	0.975546
$d\bar{d} \to \bar{d}dgg$	0.902231	0.902215
$u\bar{d} \to \bar{d}u\bar{s}s$	0.0116469	0.0116467
$u\bar{d} \to \bar{d}u\bar{u}u$	0.0524928	0.0524927
$d\bar{d} \to \bar{d}d\bar{d}d$	0.0583822	0.0583821
$u\bar{d} \to \bar{d}u\bar{s}gs$	0.000453678	0.000453671
$u\bar{d} \to \bar{d}u\bar{u}gu$	0.00202449	0.00202446

Table 2. CPU time in seconds for the computation of some matrix elements summed over all helicities and colours on a standard PC (Pentium IV with 2 GHz). The examples consist of the n gluon amplitudes, the amplitudes with a $\bar{q}, q$-pair and $(n-2)$ gluons and the amplitudes with two distinct $\bar{q}, q$-pairs and $(n-4)$ gluons

n	4	5	6	7	8
time for $\|\mathcal{A}(g_1, ..., g_n)\|^2$	0.0006	0.009	0.18	4	127
time for $\|\mathcal{A}(\bar{q}, q, g_3, ..., g_n)\|^2$	0.0004	0.003	0.05	0.6	14
time for $\|\mathcal{A}(\bar{q}, q, \bar{q}', q', g_5, ..., g_n)\|^2$	0.0002	0.002	0.02	0.4	8

Table 2 gives an indication for the CPU time needed to evaluate matrix elements of increasing complexity. It gives the CPU time needed for the computation of the matrix elements, summed over all colours and spins, corresponding to the following cases: The amplitude $\mathcal{A}(g_1, ..., g_n)$ with n gluons, the amplitude $\mathcal{A}(\bar{q}, q, g_3, ..., g_n)$ with an $\bar{q}, q$-pair and $(n-2)$ gluons and the amplitude $\mathcal{A}(\bar{q}, q, \bar{q}', q', g_5, ..., g_n)$ with two distinct $\bar{q}, q$-pairs and $(n-4)$ gluons.

5 Conclusions and outlook

In this paper I discussed an algorithm for the automated computation of spin- and colour-correlated Born matrix elements in QCD. These matrix elements are needed for NLO calculations in combination with the subtraction method. I implemented the algorithm into a computer program. The program handles QCD amplitudes with massless and/or massive quarks. In addition, I have implemented the extension to QCD amplitudes with one additional electro-weak boson.

The methods presented here are part of a larger project for the automated computation of observables at next-to-leading order for LHC physics. The remaining missing piece is the automated computation of the interference term of the one-loop amplitude with the Born amplitude. In a previous publication, we already reported on the automated computation of the one-loop integrals entering the one-loop amplitude [31]. Work on the automated computation of the interference term is in progress.

Appendix A: Feynman rules

In this appendix I summarise the colour-ordered Feynman rules. I extract from each formula the coupling constant and split the remainder into a colour part and a kinematical part.

A.1 Propagators, polarisation vectors and polarisation sums

Gluon propagator

In Feynman gauge, the gluon propagator is given by $-\mathrm{i}g^{\mu\nu}\delta^{ab}/k^2$. Contraction of the kinematical part $-\mathrm{i}g^{\mu\nu}/k^2$ with $(1/2)\bar{\sigma}^{\mu\dot{B}A}\bar{\sigma}^{\nu\dot{D}C}$ yields

$$P^{\dot{B}A\dot{D}C}(k) = \quad \dot{B}A \,\underleftarrow{\text{\small 00000}}\, \dot{D}C$$
$$= \frac{\mathrm{i}}{k^2}\left(-\varepsilon^{\dot{B}\dot{D}}\varepsilon^{AC}\right). \tag{A.1}$$

The colour factor δ^{ab} is contracted within the double-line notation with $\sqrt{2}T^a_{ij}\sqrt{2}T^b_{kl}$:

$$\sqrt{2}T^a_{ij}\,\delta^{ab}\,\sqrt{2}T^b_{kl} = \delta_{il}\delta_{kj} - \frac{1}{N}\delta_{ij}\delta_{kl}. \tag{A.2}$$

The colour structure is split into two pieces. The first piece $\delta_{il}\delta_{kj}$ corresponds to the propagation of a $U(N)$ gluon, whereas the second piece $-\delta_{ij}\delta_{kl}/N$ subtracts out the additional $U(1)$ gluon. Schematically we have

$$\begin{aligned} {}^i_j \xrightarrow{\qquad} {}^l_k &= \delta_{il}\delta_{kj}, \\ {}^i_j \dashleftarrow\!\dashrightarrow {}^l_k &= -\frac{1}{N}\delta_{ij}\delta_{kl}. \end{aligned} \tag{A.3}$$

Note that each propagation of a $U(1)$ gluon is accompanied by a factor $(-1)/N$.

Quark propagator

The kinematical piece of the quark propagator reads

$$\frac{\mathrm{i}}{\not{p}-m} \tag{A.4}$$

The colour factor is simply

$$i \xleftarrow{\qquad} j \ = \delta_{ij}. \tag{A.5}$$

Gluon polarisation vectors and colour projector

The gluon polarisation vectors are given by

$$\varepsilon_+^{\dot{A}B}(k,q) = \frac{1}{\langle qk\rangle}\,k^{\dot{A}}q^B, \quad \varepsilon_-^{\dot{A}B}(k,q) = \frac{1}{[kq]}\,q^{\dot{A}}k^B. \tag{A.6}$$

k is the momentum of the gluon and q is an arbitrary light-like reference momentum. The dependence on q drops out in gauge-invariant quantities.

As for the colour factor, in the conventional approach we sum for the squared matrix element for each gluon over all eight colour degrees of freedom. In the double-line notation a factor $\sqrt{2}T^a_{ij}$ is moved at each end into the colour projector. Therefore, the colour projector reads

$$\sqrt{2}T^a_{ij}\ \sqrt{2}T^a_{kl} = \delta_{il}\delta_{kj} - \frac{1}{N}\delta_{ij}\delta_{kl}. \tag{A.7}$$

A.2 Vertices

Quark–gluon vertex

The kinematical part of the quark–gluon vertex is given by

$$= -\mathrm{i}\sqrt{2}\varepsilon_{CA}\varepsilon_{\dot{D}\dot{B}},$$

$$= -\mathrm{i}\sqrt{2}\delta_C{}^B\delta_{\dot{D}}{}^{\dot{A}}. \tag{A.8}$$

The colour factor is given by

$$= \frac{1}{\sqrt{2}}\delta_{il}\delta_{kj}. \tag{A.9}$$

Here I neglected terms proportional to δ_{kl}, which vanish when contracted into the gluon propagator or the colour projector of (A.7).

Three gluon vertex

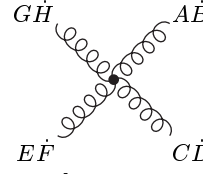The kinematical part of the three-gluon vertex is given by

$$= \frac{\mathrm{i}}{\sqrt{2}}\left[\varepsilon_{CE}\varepsilon_{\dot{D}\dot{F}}\left(k_3-k_2\right)_{A\dot{B}} + \varepsilon_{EA}\varepsilon_{\dot{F}\dot{B}}\left(k_1-k_3\right)_{C\dot{D}}\right.$$
$$\left. + \varepsilon_{AC}\varepsilon_{\dot{B}\dot{D}}\left(k_2-k_1\right)_{E\dot{F}}\right]. \tag{A.10}$$

The colour factor reads

$$= \frac{1}{\sqrt{2}}\delta_{i_1 j_2}\delta_{i_2 j_3}\delta_{i_3 j_1}. \tag{A.11}$$
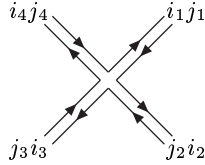
Four gluon vertex

The kinematical part of the four-gluon vertex is given by

$$= 2\mathrm{i}\left[2\varepsilon_{AE}\varepsilon_{\dot{B}\dot{F}}\varepsilon_{CG}\varepsilon_{\dot{D}\dot{H}} - \varepsilon_{AC}\varepsilon_{\dot{B}\dot{D}}\varepsilon_{EG}\varepsilon_{\dot{F}\dot{H}} - \varepsilon_{AG}\varepsilon_{\dot{B}\dot{H}}\varepsilon_{CE}\varepsilon_{\dot{D}\dot{F}}\right]. \quad (A.12)$$

The colour factor reads

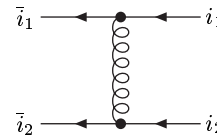$$= \frac{1}{2}\delta_{i_1 j_2}\delta_{i_2 j_3}\delta_{i_3 j_4}\delta_{i_4 j_1}. \quad (A.13)$$

Appendix B: Colour correlations

In this appendix I list all colour-correlation operators $\mathbf{T}_a \cdot \mathbf{T}_b$ between two partons in the double line notation.

$$\mathcal{A}^*\left(...a,...,b,...\right)\left(\mathbf{T}_a \cdot \mathbf{T}_b\right)\mathcal{A}\left(...a,...,b,...\right). \quad (B.1)$$
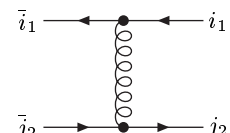
Their action between amplitudes is defined in (6) and (7). As we write all amplitudes in the colour-flow decomposition, we would like to know the action of these operators in this basis. In the following I denote the colour indices of the amplitude $\mathcal{A}^*$ with barred indices, the colour indices of the amplitude $\mathcal{A}$ with un-barred indices.
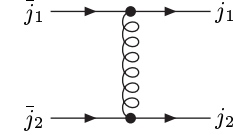
Quark–quark $(\mathbf{T}_q \cdot \mathbf{T}_q)$

$$= \frac{1}{2}\left(\delta_{\bar{i}_1 i_2}\delta_{\bar{i}_2 i_1} - \frac{1}{N}\delta_{\bar{i}_1 i_1}\delta_{\bar{i}_2 i_2}\right). \quad (B.2)$$
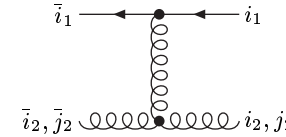
Quark–antiquark $(\mathbf{T}_q \cdot \mathbf{T}_{\bar{q}})$

$$= -\frac{1}{2}\left(\delta_{\bar{i}_1 \bar{j}_2}\delta_{j_2 i_1} - \frac{1}{N}\delta_{\bar{i}_1 i_1}\delta_{j_2 \bar{j}_2}\right). \quad (B.3)$$

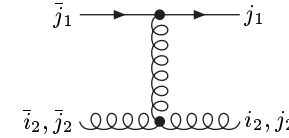**Antiquark–antiquark $(\mathbf{T}_{\bar{q}} \cdot \mathbf{T}_{\bar{q}})$**

$$= \frac{1}{2}\left(\delta_{j_1 \bar{j}_2}\delta_{j_2 \bar{j}_1} - \frac{1}{N}\delta_{j_1 \bar{j}_1}\delta_{j_2 \bar{j}_2}\right). \quad (B.4)$$
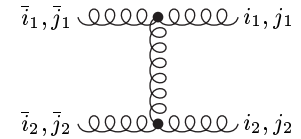
Quark–gluon $(\mathbf{T}_q \cdot \mathbf{T}_g)$

$$= \frac{1}{2}\left(\delta_{\bar{i}_1 i_2}\delta_{\bar{i}_2 i_1}\delta_{j_2 \bar{j}_2} - \delta_{\bar{i}_1 \bar{j}_2}\delta_{j_2 i_1}\delta_{\bar{i}_2 i_2}\right). \quad (B.5)$$

Antiquark–gluon $(\mathbf{T}_{\bar{q}} \cdot \mathbf{T}_g)$

$$= \frac{1}{2}\left(\delta_{j_1 \bar{j}_2}\delta_{j_2 \bar{j}_1}\delta_{\bar{i}_2 i_2} - \delta_{j_1 i_2}\delta_{\bar{i}_2 \bar{j}_1}\delta_{j_2 \bar{j}_2}\right). \quad (B.6)$$

Gluon–gluon $(\mathbf{T}_g \cdot \mathbf{T}_g)$

$$= \frac{1}{2}\left(\delta_{\bar{i}_1 i_1}\delta_{\bar{i}_2 i_2}\delta_{j_1 \bar{j}_2}\delta_{j_2 \bar{j}_1} - \delta_{\bar{i}_1 i_1}\delta_{j_2 \bar{j}_2}\delta_{j_1 i_2}\delta_{\bar{i}_2 \bar{j}_1}\right.$$
$$\left. -\delta_{j_1 \bar{j}_1}\delta_{\bar{i}_2 i_2}\delta_{\bar{i}_1 \bar{j}_2}\delta_{j_2 i_1} + \delta_{j_1 \bar{j}_1}\delta_{j_2 \bar{j}_2}\delta_{\bar{i}_1 i_2}\delta_{\bar{i}_2 i_1}\right). \quad (B.7)$$

Appendix C: Details on the implementation

In this appendix I provide some details on the implementation of the algorithm into a C++ program. I will discuss in a small example how the colour algebra is performed. I will also give some hints on the implementation of loops over multi-indices like permutation, partitions, etc.

C.1 Colour algebra

Below I show a small program, which defines the colour structures

$$c_1 = \delta_{i_1 j_2} \delta_{i_2 j_1}, \ \ c_1^\dagger = \delta_{j_2 i_1} \delta_{j_1 i_2} \tag{C.1}$$

and contracts them:

$$c_{11} = c_1 c_1^\dagger. \tag{C.2}$$

The result is obviously $c_{11} = N^2$, which equals 9 for $N = 3$.

```
#include <iostream>

#include ''ginac/ginac.h''

int main()

{
using namespace GiNaC;

// number of colours
int Nc = 3;

// define colour indices
ex i1 = idx( symbol("i1"), Nc );
ex i2 = idx( symbol("i2"), Nc );

ex j1 = idx( symbol("j1"), Nc );
ex j2 = idx( symbol("j2"), Nc );

// define colour structures
ex c1 = delta_tensor(i1,j2)*delta_tensor(i2,j1);
ex c1_conj = delta_tensor(j2,i1)*delta_tensor(j1,i2);

// square it and contract indices
ex c11 = c1_conj * c1;
c11 = c11.simplify_indexed();

// convert the result to a ''double'' variable
double c_double = real(ex_to<numeric>( c11 )).to_double();

std::cout << ''result = '' << c_double << std::endl;

return 0;
}
```

C.2 Summing over multi-indices

The algorithms involves the summation over multi-indices. A rather simple example for a multi-index would be a k-tuple $(i_0, i_1, ..., i_{k-1})$ where each entry can take values from 0 to $N-1$. Other examples are the sum over permutations of k elements as in (34) or the multi-index in (45). To make the code readable it is desirable to write the loop as

```
{
int N = 7;
int k = 3;

multi_index i_multi(N,k);

for( i_multi.init(); !i_multi.overflow(); i_multi++)
{
// can use i_multi[0], i_multi[1], etc. here
}
}
```

and to hide the details on how the multi-index is increased into a separate class. A possible header file for the class `multi_index` could look as follows:

```
class multi_index {

public :
multi_index(size_t N, size_t k);

// functions
multi_index & init(void); // initialisation
bool overflow(void) const; // returns overflow flag
multi_index & operator++ (int); // postfix increment
size_t operator[](size_t i) const; // subscripting

// member variables :
protected :
size_t N;
std::vector<size_t> v;
bool flag_overflow;
};
```

This class contains a method `init` to initialise the multi-index to the first value, an operator `++` which increases the multi-index to the next value, and method `overflow`, which returns true if all values have been run through.

References

1. F.A. Berends, W.T. Giele, Nucl. Phys. B **306**, 759 (1988)
2. F.A. Berends, W.T. Giele, H. Kuijf, Phys. Lett. B **232**, 266 (1989)
3. F.A. Berends, H. Kuijf, B. Tausk, W.T. Giele, Nucl. Phys. B **357**, 32 (1991)
4. F. Caravaglios, M. Moretti, Phys. Lett. B **358**, 332 (1995), hep-ph/9507237
5. F. Caravaglios, M.L. Mangano, M. Moretti, R. Pittau, Nucl. Phys. B **539**, 215 (1999), hep-ph/9807570
6. P. Draggiotis, R.H.P. Kleiss, C.G. Papadopoulos, Phys. Lett. B **439**, 157 (1998), hep-ph/9807207
7. P.D. Draggiotis, R.H.P. Kleiss, C.G. Papadopoulos, Eur. Phys. J. C **24**, 447 (2002), hep-ph/0202201
8. T. Stelzer, W.F. Long, Comput. Phys. Commun. **81**, 357 (1994), hep-ph/9401258
9. A. Pukhov et al. (1999), hep-ph/9908288
10. F. Yuasa et al., Prog. Theor. Phys. Suppl. **138**, 18 (2000), hep-ph/0007053
11. F. Krauss, R. Kuhn, G. Soff, JHEP **02**, 044 (2002), hep-ph/0109036
12. W.B. Kilgore, W.T. Giele, Phys. Rev. D **55**, 7183 (1997), hep-ph/9610433
13. Z. Nagy, Phys. Rev. Lett. **88**, 122003 (2002), hep-ph/0110315
14. Z. Nagy, Phys. Rev. D **68**, 094002 (2003), hep-ph/0307268
15. J. Campbell, R.K. Ellis, Phys. Rev. D **65**, 113007 (2002), hep-ph/0202176
16. W. Beenakker et al., Nucl. Phys. B **653**, 151 (2003), hep-ph/0211352
17. S. Dawson, C. Jackson, L.H. Orr, L. Reina, D. Wackeroth, Phys. Rev. D **68**, 034022 (2003), hep-ph/0305087
18. V. Del Duca, W. Kilgore, C. Oleari, C. Schmidt, D. Zeppenfeld, Phys. Rev. Lett. **87**, 122001 (2001), hep-ph/0105129
19. V. Del Duca, W. Kilgore, C. Oleari, C. Schmidt, D. Zeppenfeld, Nucl. Phys. B **616**, 367 (2001), hep-ph/0108030
20. D.E. Soper, Phys. Rev. Lett. **81**, 2638 (1998), hep-ph/9804454
21. D.E. Soper, Phys. Rev. D **62**, 014009 (2000), hep-ph/9910292

22. G. Passarino, Nucl. Phys. B **619**, 257 (2001), hep-ph/0108252
23. A. Ferroglia, M. Passera, G. Passarino, S. Uccirati, Nucl. Phys. B **650**, 162 (2003), hep-ph/0209219
24. Z. Nagy, D.E. Soper, JHEP **09**, 055 (2003), hep-ph/0308127
25. A. Denner, S. Dittmaier, Nucl. Phys. B **658**, 175 (2003), hep-ph/0212259
26. S. Dittmaier, Nucl. Phys. B **675**, 447 (2003), hep-ph/0308246
27. W.T. Giele, E.W.N. Glover, JHEP **04**, 029 (2004), hep-ph/0402152
28. R.K. Ellis, W.T. Giele, G. Zanderighi (2005), hep-ph/0508308
29. F. del Aguila, R. Pittau, JHEP **07**, 017 (2004), hep-ph/0404120
30. R. Pittau (2004), hep-ph/0406105
31. A. van Hameren, J. Vollinga, S. Weinzierl, Eur. Phys. J. C **41**, 361 (2005), hep-ph/0502165
32. T. Binoth, G. Heinrich, N. Kauer, Nucl. Phys. B **654**, 277 (2003), hep-ph/0210023
33. T. Binoth, J.P. Guillet, G. Heinrich, E. Pilon, C. Schubert (2005), hep-ph/0504267
34. A. van Hameren, C.G. Papadopoulos, Acta Phys. Polon. B **35**, 2601 (2004), hep-ph/0410189
35. W.T. Giele, E.W.N. Glover, Phys. Rev. D **46**, 1980 (1992)
36. W.T. Giele, E.W.N. Glover, D.A. Kosower, Nucl. Phys. B **403**, 633 (1993), hep-ph/9302225
37. S. Keller, E. Laenen, Phys. Rev. D **59**, 114004 (1999), hep-ph/9812415
38. S. Frixione, Z. Kunszt, A. Signer, Nucl. Phys. B **467**, 399 (1996), hep-ph/9512328
39. S. Catani, M.H. Seymour, Nucl. Phys. B **485**, 291 (1997), hep-ph/9605323
40. S. Catani, M.H. Seymour, Nucl. Phys. B **510**, 503 (1997), Erratum
41. S. Dittmaier, Nucl. Phys. B **565**, 69 (2000), hep-ph/9904440
42. L. Phaf, S. Weinzierl, JHEP **04**, 006 (2001), hep-ph/0102207
43. S. Catani, S. Dittmaier, M.H. Seymour, Z. Trocsanyi, Nucl. Phys. B **627**, 189 (2002), hep-ph/0201036
44. C. Bauer, A. Frink, R. Kreckel, J. Symbolic Computation **33**, 1 (2002), cs.sc/0004015
45. F.A. Berends, R. Kleiss, P. De Causmaecker, R. Gastmans, T.T. Wu, Phys. Lett. B **103**, 124 (1981)
46. P. De Causmaecker, R. Gastmans, W. Troost, T.T. Wu, Nucl. Phys. B **206**, 53 (1982)
47. J.F. Gunion, Z. Kunszt, Phys. Lett. B **161**, 333 (1985)
48. Z. Xu, D.-H. Zhang, L. Chang, Nucl. Phys. B **291**, 392 (1987)
49. R. Gastmans, T.T. Wu, (Clarendon, Oxford 1990) 648 p. (International series of monographs on physics, 80)
50. P. Cvitanovic, P.G. Lauwers, P.N. Scharbach, Nucl. Phys. B **186**, 165 (1981)
51. F.A. Berends, W. Giele, Nucl. Phys. B **294**, 700 (1987)
52. M.L. Mangano, S.J. Parke, Z. Xu, Nucl. Phys. B **298**, 653 (1988)
53. D. Kosower, B.-H. Lee, V.P. Nair, Phys. Lett. B **201**, 85 (1988)
54. Z. Bern, D.A. Kosower, Nucl. Phys. B **362**, 389 (1991)
55. V. Del Duca, L.J. Dixon, F. Maltoni, Nucl. Phys. B **571**, 51 (2000), hep-ph/9910563
56. F. Maltoni, K. Paul, T. Stelzer, S. Willenbrock, Phys. Rev. D **67**, 014026 (2003), hep-ph/0209271
57. D.A. Kosower, Nucl. Phys. B **335**, 23 (1990)
58. F. Cachazo, P. Svrcek, E. Witten, JHEP **09**, 006 (2004), hep-th/0403047
59. R. Britto, F. Cachazo, B. Feng (2004), hep-th/0412308
60. I. Bena, Z. Bern, D.A. Kosower (2004), hep-th/0406133
61. C. Schwinn, S. Weinzierl, JHEP **05**, 006 (2005), hep-th/0503015
62. G. 't Hooft, Nucl. Phys. B **72**, 461 (1974)
63. J. van der Heide, E. Laenen, L. Phaf, S. Weinzierl, Phys. Rev. D **62**, 074025 (2000), hep-ph/0003318
64. S. Weinzierl, D.A. Kosower, Phys. Rev. D **60**, 054028 (1999), hep-ph/9901277
65. A. Brandenburg, S. Dittmaier, P. Uwer, S. Weinzierl, Nucl. Phys. Proc. Suppl. **135**, 71 (2004), hep-ph/0408137